

Human Fbh1 helicase contributes to genome maintenance via pro- and anti-recombinase activities

Kasper Fugger,¹ Martin Mistrik,² Jannie Rendtew Danielsen,¹ Christoffel Dinant,¹ Jacob Falck,¹ Jiri Bartek,^{1,2} Jiri Lukas,¹ and Niels Mailand¹

¹Institute of Cancer Biology and Center for Genotoxic Stress Research, Danish Cancer Society, DK-2100 Copenhagen, Denmark

²Laboratory of Genomic Integrity, Palacky University, 783 71 Olomouc, Czech Republic

Homologous recombination (HR) is essential for faithful repair of DNA lesions yet must be kept in check, as unrestrained HR may compromise genome integrity and lead to premature aging or cancer. To limit unscheduled HR, cells possess DNA helicases capable of preventing excessive recombination. In this study, we show that the human Fbh1 (hFbh1) helicase accumulates at sites of DNA damage or replication stress in a manner dependent fully on its helicase activity and partially on its conserved F box. hFbh1 interacted with single-stranded DNA (ssDNA), the formation of which was

required for hFbh1 recruitment to DNA lesions. Conversely, depletion of endogenous Fbh1 or ectopic expression of helicase-deficient hFbh1 attenuated ssDNA production after replication block. Although elevated levels of hFbh1 impaired Rad51 recruitment to ssDNA and suppressed HR, its small interfering RNA-mediated depletion increased the levels of chromatin-associated Rad51 and caused unscheduled sister chromatid exchange. Thus, by possessing both pro- and anti-recombinogenic potential, hFbh1 may cooperate with other DNA helicases in tightly controlling cellular HR activity.

Introduction

Genome integrity is constantly challenged by DNA damage, resulting from a range of genotoxic insults. DNA double-strand breaks (DSBs) represent the most toxic chromosomal lesion, arising from a variety of sources such as ionizing radiation (IR) or collapsed replication forks. To counteract the potentially deleterious effects of DSBs, cells have evolved homologous recombination (HR)-based repair mechanisms capable of restoring genomic integrity in an error-free manner and that rely on the availability of an undamaged homologous sister chromatid as a template for the repair process.

A key event in HR repair is the formation of a nucleofilament of the rate-limiting recombinase Rad51, wrapped around single-stranded DNA (ssDNA) generated in the vicinity of the DSB (San Filippo et al., 2008). The Rad51/ssDNA nucleofilament catalyzes

a search for a homologous sequence on the sister chromatid and promotes DNA strand invasion to initiate the repair process. Despite its importance for preserving genomic integrity, HR repair must be tightly controlled. Unrestricted HR activity is a hallmark of genetic disorders such as Bloom (BLM) and Werner syndromes, both of which display a hyper-recombination phenotype and genomic instability (Sung and Klein, 2006; Branzei and Foiani, 2007). To restrict HR, cells harbor proteins termed anti-recombinases. In budding yeast, the Srs2 helicase has such a function, preventing spontaneous and unscheduled HR by dismantling Rad51 from ssDNA (Krejci et al., 2003; Veaute et al., 2003). In humans, the genes mutated in BLM, Werner, and Rothmund-Thomson (RecQL4) syndromes also encode helicases belonging to the RecQ family, all of which exhibit anti-recombinase activity (Wu and Hickson, 2006). BLM dissociates Rad51/ssDNA nucleofilaments, thereby suppressing HR, a function that was also reported for the helicase RecQL5 (Bugreev et al., 2007; Hu et al., 2007).

Correspondence to Jiri Lukas: jil@cancer.dk

J. Falck's present address is Novo Nordisk A/S, DK-2880 Bagsvaerd, Denmark.

Abbreviations used in this paper: BLM, Bloom; DOX, doxycycline; DSB, double-strand break; dsDNA, double-stranded DNA; EMSA, electrophoretic mobility shift assay; hFbh1, human Fbh1; HR, homologous recombination; HU, hydroxyurea; IR, ionizing radiation; RPA, replication protein A; SCE, sister chromatid exchange; ssDNA, single-stranded DNA; WT, wild type.

© 2009 Fugger et al. This article is distributed under the terms of an Attribution-Noncommercial-Share Alike-No Mirror Sites license for the first six months after the publication date [see <http://www.jcb.org/misc/terms.shtml>]. After six months it is available under a Creative Commons License [Attribution-Noncommercial-Share Alike 3.0 Unported license, as described at <http://creativecommons.org/licenses/by-nc-sa/3.0/>].

The existence of several helicases with anti-recombinogenic properties in mammalian cells suggests a considerable degree of complexity and redundancy in HR regulation. Recently, a functional homologue of *Saccharomyces cerevisiae* Srs2, RTEL1, was identified in humans (Barber et al., 2008). Fbh1, another conserved helicase with similarity to Srs2, has also been proposed to be a functional homologue of Srs2 in fission yeast and higher eukaryotes (Chiolo et al., 2007), but so far little is known about the function of Fbh1. Fbh1 belongs to the UvrD family of helicases and has 3'–5' DNA-unwinding activity (Kim et al., 2004). Moreover, Fbh1 is a putative E3 ubiquitin ligase by virtue of a conserved F box, enabling it to potentially function as an adaptor for the Skp, Cullin, F box-containing complex (Kim et al., 2004). However, at present, its ubiquitylation targets are unknown. In *Schizosaccharomyces pombe*, Fbh1 knockout leads to increased sensitivity to DNA-damaging agents (Morishita et al., 2005; Osman et al., 2005). Chicken DT40 cells ablated for Fbh1 exhibit an overall mild phenotype yet display an elevated rate of sister chromatid exchange (SCE), which is a phenomenon associated with hyper recombination (Kohzaki et al., 2007). In these cells, Fbh1 acts redundantly with BLM, and their codisruption causes a synergistic increase in DNA damage sensitivity.

In this study, we have performed a detailed analysis of the functional properties of Fbh1 in human cells. We show that human Fbh1 (hFbh1) possesses both pro- and anti-recombinogenic activities, contributing to the regulation of ssDNA production at replication blocks as well as regulation of Rad51 nucleofilament formation and HR repair. Our findings reveal evolutionary conservancy of Fbh1 function and broaden the spectrum of anti-recombinogenic helicases in mammalian cells.

Results and discussion

hFbh1 accumulates at sites of DNA damage

To investigate whether Fbh1 plays a role in the DNA damage response in human cells, we examined the impact of DNA-damaging insults on the subcellular localization of hFbh1. Because high levels of hFbh1 appeared toxic to cells (unpublished data), we generated a U2OS cell line stably expressing GFP-tagged hFbh1 in a doxycycline (DOX)-inducible fashion at low levels, which did not detectably interfere with cell proliferation (Fig. S1 A). In this cell line, GFP-hFbh1 showed uniform nuclear staining upon induction in the absence of exogenous DNA damage (Fig. 1 A). However, in response to DSBs generated by IR or laser microirradiation or replication blocks elicited by treatment with hydroxyurea (HU), GFP-hFbh1 accumulated in discrete subnuclear foci (Fig. 1 A), which is similar to the behavior of a range of DNA damage-responsive proteins. The GFP-hFbh1 foci completely colocalized with the ssDNA-binding protein replication protein A (RPA) but only partially overlapped with γ -H2AX, a marker for DSBs (Fig. 1 A). The formation of GFP-hFbh1 foci in response to IR was restricted to S and G2 phases, the cell cycle stages permissive for HR, as their formation occurred only in cyclin A-positive cells and included BrdU-incorporating S phase cells (Fig. 1 B). In response to HU,

the kinetics of GFP-hFbh1 focus formation paralleled that of RPA, becoming apparent \sim 30 min after exposure to the drug (Fig. 1 C). Similar kinetics of GFP-hFbh1 recruitment was observed in response to IR (Fig. S1 B). These observations suggest that hFbh1 is a novel factor involved in the DNA damage response in human cells, functioning at an advanced stage associated with ssDNA formation.

hFbh1 interacts with ssDNA

The recruitment of RecQ helicases to DNA lesions can be highly dependent on specific DNA structures produced during the process of HR (Wu and Hickson, 2006). To investigate the requirements for hFbh1 recruitment to DNA lesions, we first assessed the impact of depleting different proteins involved in processing damaged DNA. Knockdown of CtIP, a factor required for resection of DSBs into ssDNA (Sartori et al., 2007), severely impaired GFP-hFbh1 focus formation in response to IR but not HU (Fig. 2 A), which generates ssDNA independent of resection. This suggested that hFbh1 is recruited to ssDNA but not unprocessed DSBs. To determine whether hFbh1 recruitment to damaged DNA required DNA intermediates produced after strand invasion during HR, we depleted Rad51 or Rad51C, a Rad51 mediator essential for Rad51 focus formation after DNA damage (Rodrigue et al., 2006). Although the Rad51 and Rad51C siRNAs depleted their targets (Fig. 2 A), such treatments did not interfere with GFP-hFbh1 recruitment in response to either IR or HU (Fig. 2 A), suggesting that hFbh1 is directly recruited to ssDNA rather than recombination intermediates.

To test the idea that hFbh1 recognizes ssDNA, cells were prelabeled with BrdU before exposure to HU and subjected to immunostaining under nondenaturing conditions in which BrdU is only detectable in ssDNA regions (Groth et al., 2007). Under these conditions, GFP-hFbh1 completely colocalized with the BrdU-decorated ssDNA compartment (Fig. 2 B), supporting the notion that hFbh1 associates with ssDNA. To see whether hFbh1 directly binds ssDNA, we performed electrophoretic mobility shift assays (EMSAs) in which purified GST-hFbh1 was incubated with ssDNA or double-stranded DNA (dsDNA) probes. As shown in Fig. 2 C, hFbh1 bound to ssDNA but not to dsDNA. Although hFbh1 recruitment to ssDNA regions generated by IR was restricted to S and G2 phases, we observed that GFP-hFbh1 accumulated at UV-damaged DNA in a subset of cyclin A-negative cells (Fig. S2 A). However, we failed to detect accumulation of GFP-Fbh1 at UV lesions in early G1 cells after mitotic shake off (Fig. S2 B). We conclude from these experiments that hFbh1 may be recruited to ssDNA produced in late G1 but not in early G1.

hFbh1 displaces Rad51 from chromatin to suppress HR

Evidence from yeast and other organisms suggests that Srs2 and the RecQ helicases possess anti-recombinogenic activities by dismantling the Rad51 nucleofilament from ssDNA produced during normal replication (Sung and Klein, 2006). We tested whether hFbh1 might similarly prevent Rad51 focus formation after a replication block using the inducible GFP-hFbh1 cell line. As expected, Rad51 readily accumulated in nuclear foci when uninduced cells were treated with HU or IR (Fig. 3 A).

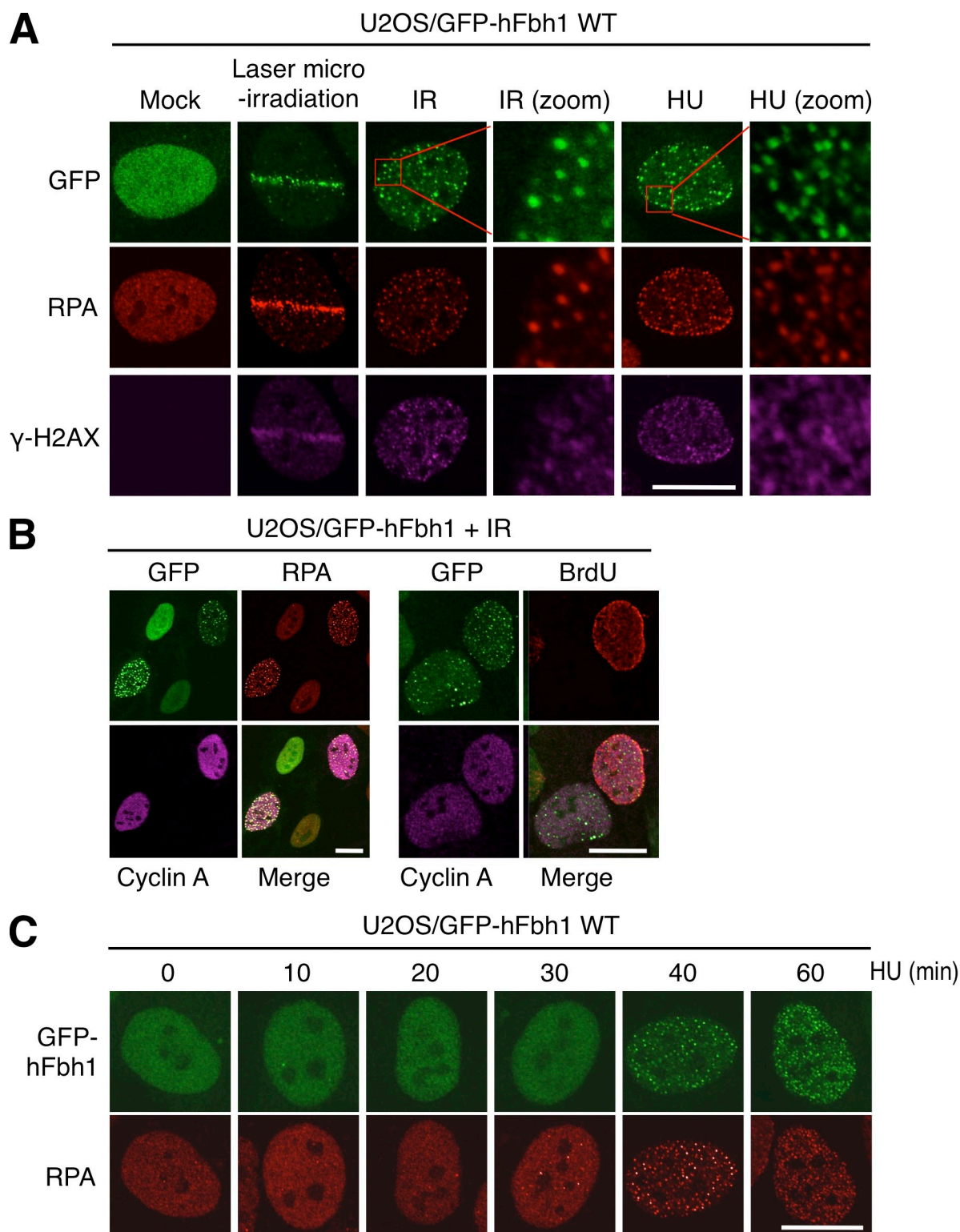


Figure 1. hFbh1 accumulates at sites of DNA damage in S and G2 phase cells. (A) U2OS/GFP-hFbh1 WT cells were induced to express GFP-hFbh1 by addition of DOX for 24 h, and were subsequently left untreated or subjected to laser microirradiation, IR (6 Gy), or HU treatment. 1 h later, the cells were fixed and coimmunostained with antibodies to RPA and γ -H2AX. Magnifications of HU- and IR-treated cells are shown (red lines). (B) U2OS/GFP-hFbh1 WT cells induced to express the transgene for 24 h were subjected to IR (6 Gy) for 1 h, pulsed with BrdU for 20 min, and fixed and coimmunostained with the indicated antibodies. (C) U2OS/GFP-hFbh1 WT cells induced with DOX for 24 h were incubated in the presence of HU for the indicated times and processed for immunofluorescence as in A. Bars, 10 μ m.

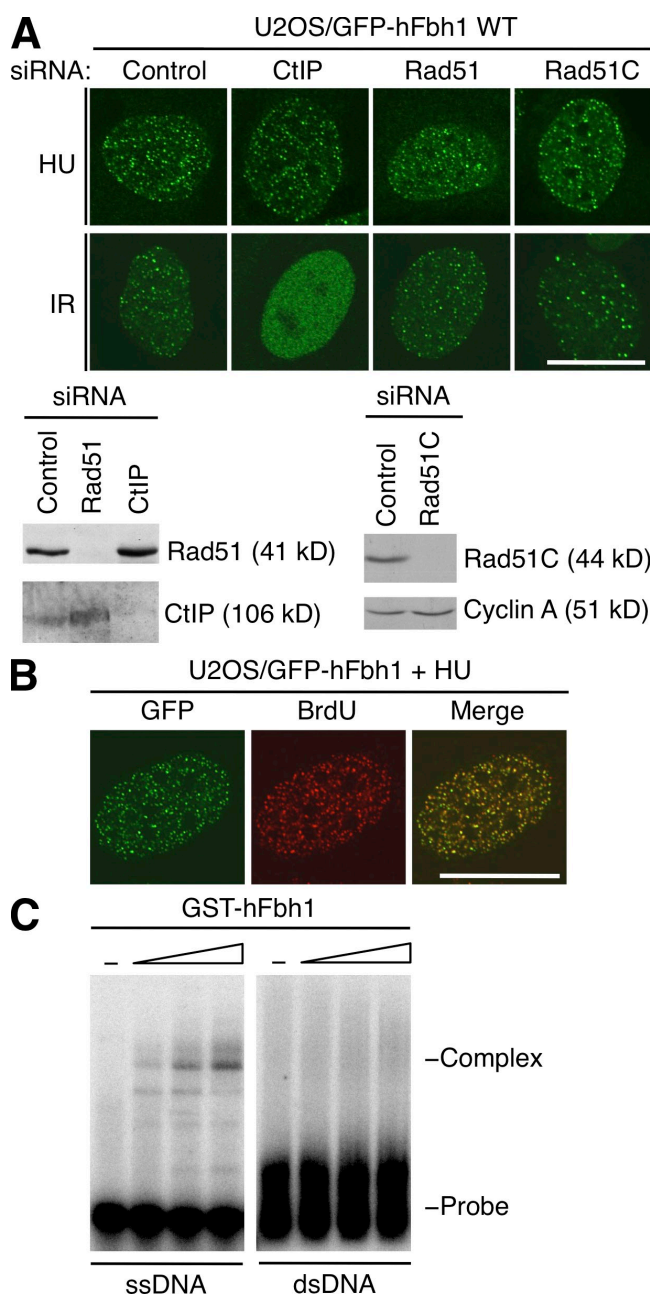


Figure 2. hFbh1 interacts with ssDNA. (A) U2OS/GFP-hFbh1 WT cells were transfected with the indicated siRNAs for 24 h, induced with DOX for an additional 24 h, and exposed to IR or HU for 1 h. (top) The cells were fixed, and the GFP signal was visualized by confocal microscopy. (bottom) Immunoblot analysis of siRNA-mediated knockdown efficiency. (B) U2OS/GFP-hFbh1 WT cells were incubated in the presence of BrdU and DOX for 24 h. The cells were treated with HU for 1 h, fixed, and immunostained with BrdU antibody under native conditions. (C) EMSA is shown. 32 P-labeled ssDNA or dsDNA probes were incubated with increasing amounts (200–1,000 nM) of GST-hFbh1 and subjected to native gel electrophoresis. Migration of the probe and the GST-hFbh1–ssDNA complex is indicated. Bars, 10 μ m.

Strikingly, however, induction of GFP-hFbh1 in these cells strongly impaired Rad51 foci formation in response to HU and IR (Fig. 3 A). Expression of Rad51 was unaffected by induction of GFP-hFbh1 (Fig. 3 B), arguing against the possibility that hFbh1, a potential E3 ubiquitin ligase, inhibits Rad51 focus

formation by targeting it for proteasomal degradation. Unlike total levels of Rad51, cellular fractionation experiments demonstrated that the HU-dependent increase in chromatin-associated Rad51 was suppressed by induction of GFP-hFbh1 (Fig. 3 B). Moreover, GFP-hFbh1 led to an increase in chromatin-bound RPA after HU treatment (Fig. 3 A), indicating that the ability of GFP-hFbh1 to prevent Rad51 accumulation at DNA damage sites did not reflect a general propensity to displace ssDNA-binding proteins. These data indicate that hFbh1 or an hFbh1-containing complex is capable of actively removing Rad51 from chromatin.

Because ectopic GFP-hFbh1 can displace Rad51 from chromatin, we speculated that depletion of endogenous hFbh1 would lead to chromatin retention of Rad51 during replication. To test this, we assessed Rad51 focus formation in primary BJ fibroblasts transfected with hFbh1 siRNAs. Using the nucleoside analogue EdU as a marker for replicating cells, we analyzed Rad51 focus formation in S phase and observed a significant, roughly threefold increase in the occurrence of spontaneous Rad51 foci in cells depleted for endogenous hFbh1 using two independent siRNAs (Fig. 3 C). To directly test whether hFbh1 has anti-recombinase activity, we used an HR reporter assay in which HR is measured as the ability of cells to repair an I-SceI-induced DSB in an inactive GFP construct that becomes functional only through HR-mediated repair (Sartori et al., 2007). We observed a marked $\sim 40\%$ decrease in HR events when hFbh1 was cotransfected with I-SceI (Fig. 3 D), which is comparable with the extent of HR suppression observed after siRNA-mediated depletion of Rad51 (not depicted). Collectively, these findings suggest that hFbh1 functions as a bona fide anti-recombination factor in human cells through its ability to dismantle the Rad51 nucleofilament and thus may help to prevent unscheduled HR during normal DNA replication and in response to DNA damage.

hFbh1 facilitates ssDNA generation at stalled replication forks

To further dissect the mechanism by which hFbh1 displaces Rad51 from chromatin, we introduced point mutations into hFbh1 to functionally impair its conserved F box (Fig. 4 A, *FB) or helicase domains (Fig. 4 A, *HL). We verified the effect of the F box mutations by demonstrating that they impaired hFbh1 binding to the Skp, Cullin, F Box-containing complex core subunit Skp1, which is the known function of the F box (Fig. S1 C). Surprisingly, hFbh1 helicase domain was also unable to bind Skp1 (Fig. S1 C), which may suggest that hFbh1 only associates stably with Skp1 in a chromatin context (see following paragraph). In agreement with data from fission yeast (Sakaguchi et al., 2008), mutation of the F box resulted in pancellular distribution of GFP-hFbh1 (unpublished data), and thus, we tagged the GFP-hFbh1 constructs with N-terminal NLSs to be able to compare their functional properties. We generated stable cell lines expressing such NLS-GFP-hFbh1 proteins and tested their ability to recruit to ssDNA regions induced by HU treatment. Although mutation of the F box partially impaired the binding of GFP-hFbh1 to RPA-coated ssDNA, disruption of the catalytic activity of its helicase domain completely prevented accumulation of GFP-hFbh1 on ssDNA (Fig. 4 B).

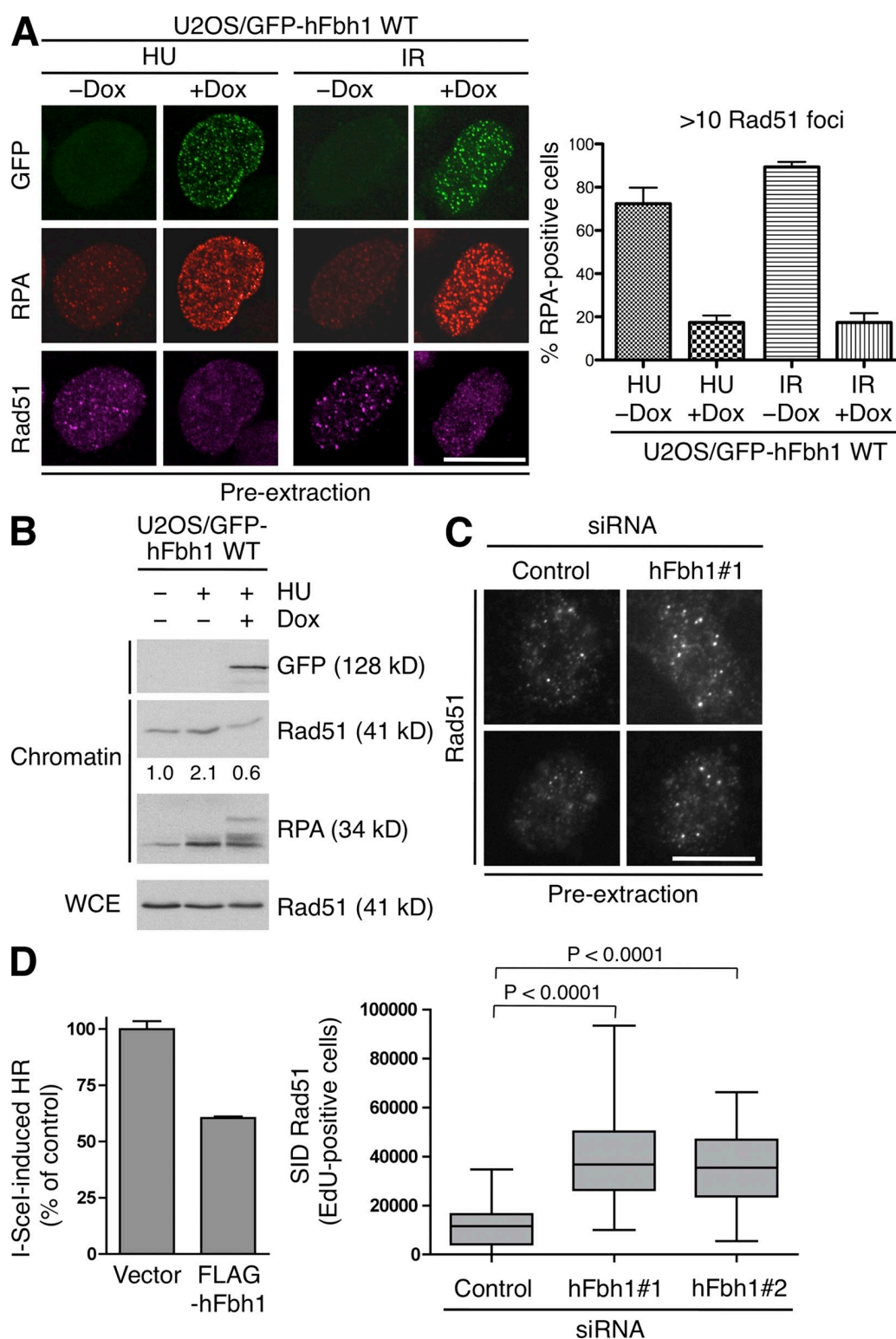


Figure 3. hFbh1 acts as an anti-recombinase by displacing Rad51 from chromatin. (A) U2OS/GFP-hFbh1 WT cells were induced or not with DOX for 24 h and subjected to HU for 2 h or IR for 1 h. (left) The cells were preextracted to remove soluble proteins, fixed, and coimmunostained with RPA and Rad51 antibodies. (right) Quantification of the results of three independent experiments is shown. (B) U2OS/GFP-hFbh1 WT cells subjected to DOX and HU treatment as in A were harvested and processed for subcellular fractionation. Chromatin-enriched fractions and whole cell extracts (WCE) were immunoblotted with the indicated antibodies. Relative intensity of the Rad51 signal is indicated. (C) BJ fibroblasts were transfected with control or two independent hFbh1 siRNAs for 48 h. (top) Cells were incubated with EdU for 30 min, preextracted, fixed, and immunostained with Rad51 antibody and EdU. Two representative fields from each transfected population are shown. (bottom) The intensity of chromatin-bound Rad51 staining was quantified by image analysis software and depicted in a box plot. SID, signal-integrated density. At least 50 EdU-positive cells were analyzed in each experiment. (D) U2OS/DR-GFP cells were transfected with plasmids encoding RFP, I-SceI, and, where indicated, empty vector or Flag-hFbh1 for 48 h. Cells were processed for flow cytometric analysis of RFP and GFP, and the extent of HR was scored as the GFP/RFP ratio. The experiment was performed in triplicates. Error bars indicate the standard deviation. Bars, 10 μ m.

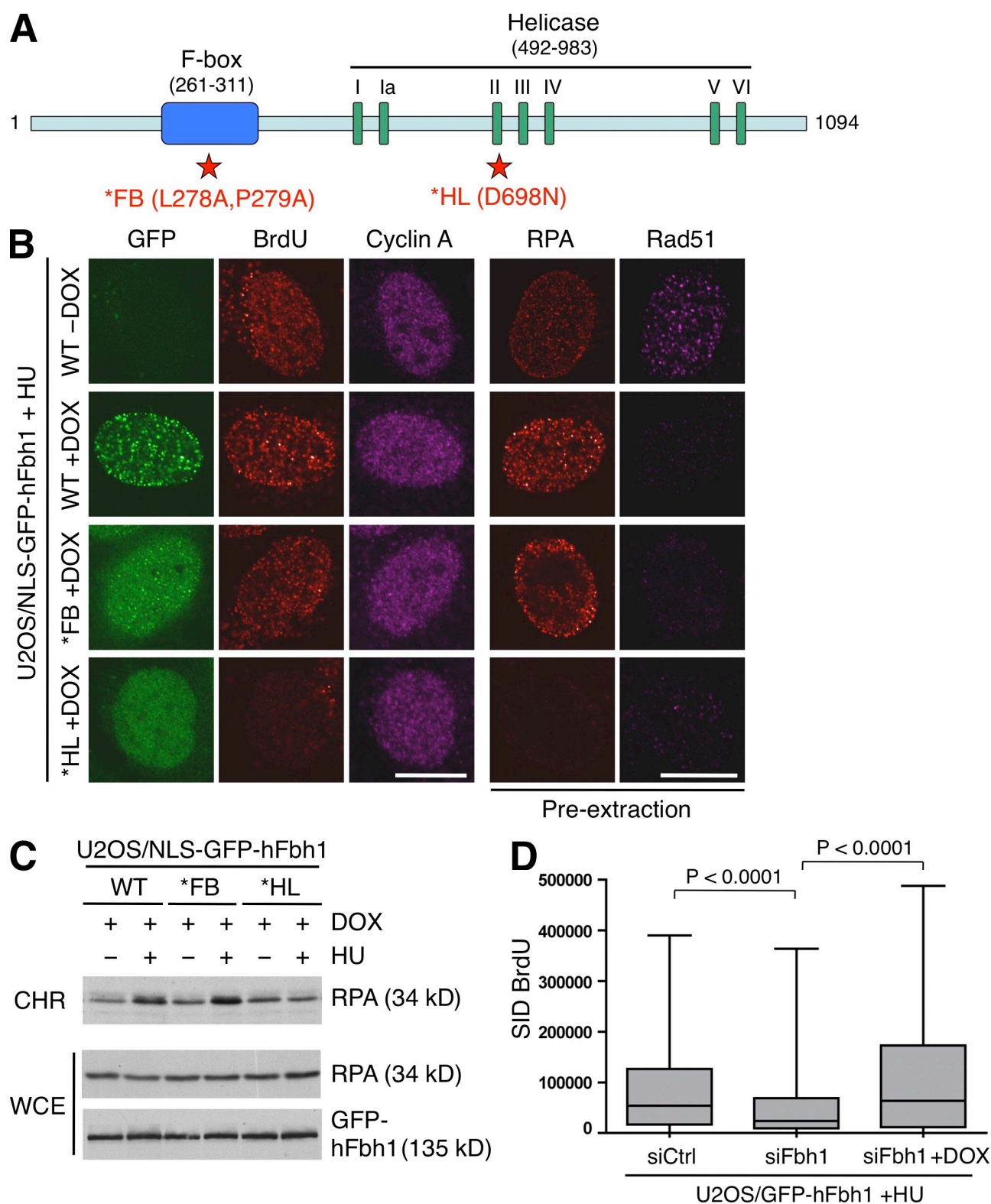


Figure 4. The helicase activity of hFbh1 facilitates ssDNA generation at replication blocks. (A) Schematic depiction of the hFbh1 protein, showing localization of conserved domains. Positions of residues mutated to generate hFbh1 F box (*FB) and helicase domain (*HL) mutants are indicated in red. (B) U2OS/NLS-GFP-hFbh1 cell lines were induced or not with DOX for 24 h, treated with HU for 1 h, and fixed. Where indicated, cells were preextracted before fixation. The cells were coimmunostained with the indicated antibodies. (C) U2OS/NLS-GFP-hFbh1 cell lines were treated with DOX and HU as in B and processed for subcellular fractionation. Chromatin-enriched fractions (CHR) or whole cell extracts (WCE) were immunoblotted with the indicated antibodies. (D) U2OS/GFP-hFbh1 cells were transfected with control or hFbh1 siRNA for 48 h and incubated in the presence of BrdU for an additional 24 h. Cells transfected with hFbh1 siRNA were either left uninduced or induced with DOX for the last 24 h. Cells were treated with HU for 2 h and processed for native fixation and immunostaining with BrdU antibody. BrdU staining was quantified by image analysis software and depicted in a box plot. SID, signal-integrated density. At least 1,000 cells were analyzed in each experiment. Bars, 10 μ m.

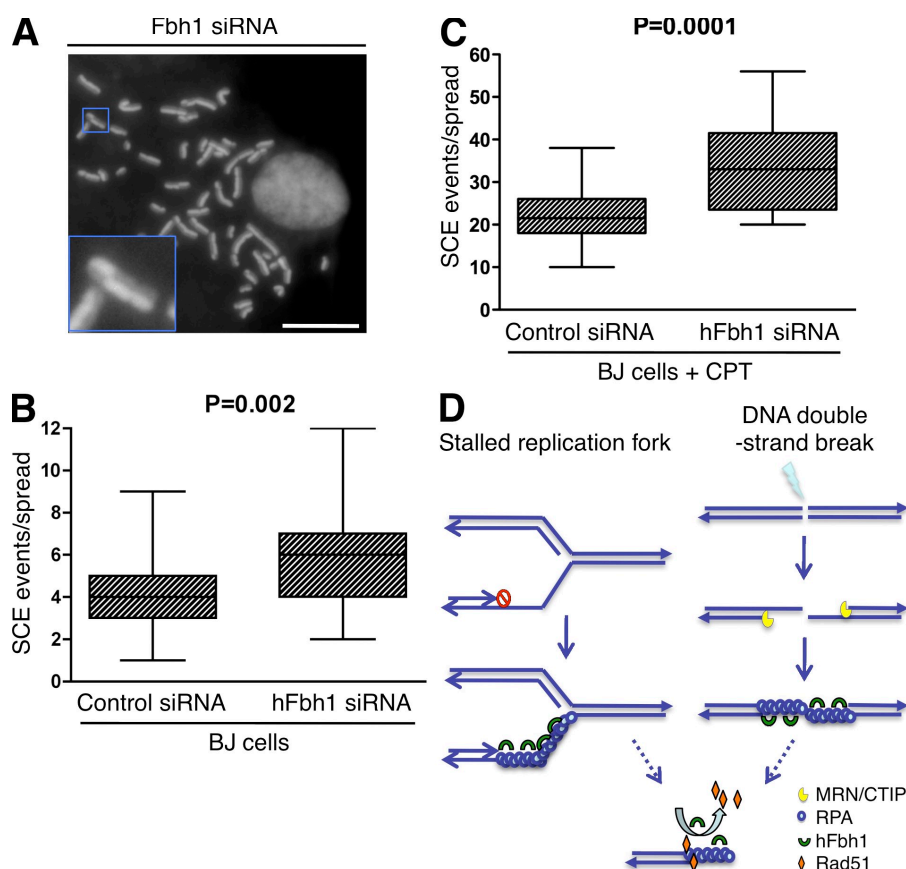


Figure 5. Depletion of hFbh1 increases SCE. (A) BJ cells were transfected with control or hFbh1 siRNAs for 48 h and subjected to SCE analysis. Metaphase chromosome spreads were prepared, and the number of SCE events was scored on a per cell basis and subjected to statistical analysis. The image shows a representative metaphase chromosome spread from hFbh1-depleted cells. The inset shows a magnification of an SCE event in the boxed region. Efficiency of hFbh1 knockdown is shown in Fig. S3. Bar, 10 μ m. (B) Box plot showing results of the experiment in A. The increase in SCE events in hFbh1-depleted cells was reproduced in an independent experiment. At least 25 metaphase spreads were analyzed in each experiment. (C) SCE assay of cells as in B. 2.5 nM camptothecin (CPT) was present in the medium throughout the course of the experiment. (D) A hypothetical model of the pro- and anti-recombinase function of hFbh1 at stalled replication forks (left) and resected DSBs (right). See Materials and methods for further details.

Surprisingly, overexpression of both F box and helicase domain mutants was still able to prevent accumulation of Rad51 at the sites of stalled replication forks (Fig. 4 B). In case of the F box mutant, this can be explained, at least in part, by its residual capability to bind damaged DNA, which might be sufficient to displace Rad51 from ssDNA. Such a scenario also indicates that the potential ubiquitin ligase activity of hFbh1 (the function of which is unknown) may not be required per se for its anti-recombinogenic function. The impact of the helicase domain mutant on Rad51 focus formation appeared more complex, and to elucidate this issue, we set out to measure the production of ssDNA after replication stress. Interestingly, we observed that cells overexpressing GFP-hFbh1 helicase domains failed to produce detectable HU-induced ssDNA stretches, which is indicated by a quantitative loss of RPA foci and reduced BrdU immunostaining under native conditions (Fig. 4 B). We obtained similar results using biochemical isolation of chromatin-enriched fractions from NLS-GFP-hFbh1-inducible cells in which the helicase domain mutant but not the wild-type (WT) or F box alleles of GFP-hFbh1 suppressed the increased chromatin loading of RPA after HU treatment (Fig. 4 C). Induction of WT or mutant GFP-hFbh1 had little impact on cell cycle distribution (Fig. S1 D), ruling out cell cycle effects as a major cause of the observed phenotypes. Using EMSA, we found that the hFbh1 helicase domain mutant retained the capability to bind to ssDNA (Fig. S2 C) even though it was not stably recruited to ssDNA sites (Fig. 4 B). Thus, it appears that by binding short stretches of ssDNA at stalled replication forks while being unable to unwind DNA, the hFbh1 helicase domain mutant may act as a

dominant-negative factor to prevent further ssDNA production in response to replication blocks, likely blocking the access of active Fbh1 (and perhaps even other ssDNA-producing helicases) to DNA lesions. As has been found for other UvrD helicases (Maluf et al., 2003), hFbh1 formed homodimers (Fig. S2 D), potentially explaining the ability of the overexpressed helicase domain mutant to act in a dominant-negative fashion in the presence of endogenous hFbh1. Thus, the lack of Rad51 focus formation observed in HU-treated cells expressing GFP-Fbh1 helicase domains (Fig. 4 B) likely reflects their inability to produce sufficiently long stretches of ssDNA required for Rad51 recruitment.

Collectively, these data suggest that in addition to its anti-recombinogenic effect, hFbh1 may also possess prorecombinase activity by facilitating ssDNA production after replication blocks to promote the loading of RPA, which is in turn required for proper checkpoint signaling and HR repair. Consistently, cells depleted for endogenous hFbh1 displayed markedly reduced ssDNA production in response to HU treatment, an effect that could be fully rescued by induction of siRNA-insensitive GFP-Fbh1 in these cells (Fig. 4 D). Such a dual role of hFbh1 in terms of pro- and anti-recombination activities is analogous to that of BLM helicase, which functions in ssDNA production after DNA damage (Gravel et al., 2008; Zhu et al., 2008) as well as displacement of Rad51 from ssDNA (Bugreev et al., 2007).

hFbh1 is a suppressor of SCE

A prominent feature of unrestricted HR is the hyper-recombination phenotype, a hallmark of BLM syndrome, which is characterized

by an increase in the SCE (Branzei and Foiani, 2007). The similar functions of hFbh1 and BLM prompted us to explore whether hFbh1 also regulates SCE. Knockdown of hFbh1 in primary fibroblasts led to a small but significant increase in SCE compared with control cells (5.6 and 4.1 events/cell, respectively; Fig. 5, A and B), an effect augmented by exposure to camptothecin (34 vs. 22 events/cell, respectively; Fig. 5 C). This is consistent with data in Fbh1-deficient chicken DT40 cells, which also exhibit increased SCE (Kohzaki et al., 2007), and further supports the notion that hFbh1 is a bonafide anti-recombinogenic factor required to restrain unscheduled HR, slight elevations of which may be sufficient to compromise genomic integrity. The existence of several helicases with anti-recombinogenic functions in human cells may account for a higher degree of redundancy in this system and could explain the relatively mild SCE phenotype observed in hFbh1 knockdown cells.

In conclusion, our findings provide evidence that hFbh1 functions as a regulator of HR repair in human cells and suggest a model of how hFbh1 exerts such a function (Fig. 5 D). In the first step, hFbh1 is recruited to genotoxic stress-induced ssDNA. By means of its helicase activity, hFbh1 may help to facilitate ssDNA production to the extent required for productive HR, and up to this stage, hFbh1 can function to promote HR initiation. However, in later stages, hFbh1 restrains excessive and/or unscheduled HR through its ability to displace Rad51 from ssDNA. Such a dual role in the multistep process of HR has also been proposed for the BLM helicase (Bugreev et al., 2007). hFbh1 may increase the pool of cellular pro- and anti-recombinase activities and thus contributes to the maintenance of genomic integrity.

Materials and methods

Plasmids and RNAi

A partial cDNA spanning amino acids 126–1,094 of hFbh1 was provided by Y.-S. Seo (Korea Advanced Institute of Science and Technology, Daejeon, Korea). The N-terminal part of hFbh1 cDNA (amino acids 1–125) was amplified from QUICK-Clone Human Universal cDNA (Clontech Laboratories, Inc.). The full-length hFbh1 was constructed by overlapping PCR of these fragments and was inserted into pEGFP-C1 (Clontech Laboratories, Inc.). From this construct, GFP-tagged hFbh1 was amplified by PCR and subcloned into pcDNA4/TO (Invitrogen) to allow DOX-inducible expression of GFP-hFbh1. To enforce nuclear expression of GFP-hFbh1, GFP-hFbh1 constructs were subcloned into pcDNA4/TO harboring three N-terminal NLSs from pCMV/Myc/nuc (Invitrogen). Introduction of point mutations to generate the F box (L278A and P279A) and helicase (D698N) mutants of hFbh1 (Osman et al., 2005) was performed using the QuikChange site-directed mutagenesis kit (Agilent Technologies). To produce GST-tagged hFbh1, full-length versions of WT or mutant hFbh1 were subcloned into pGEX-6P1 (Invitrogen). Plasmid transfections were performed using FuGene6 (Roche).

The following siRNA sequences were used in this study: hFbh1#1, 5'-GAUACAGAGUGAAGAAUGU-3'; hFbh1#2, 5'-GGGAUGUUCUUUGAUAAUU-3'; Rad51, 5'-GAGCUUGACAAACUACUUC-3'; Rad51C, 5'-GUUCAGCACUAGAUAU-3'; ChIP, 5'-GCUAAAACAGGAACGAUC-3'; and control, 5'-GCGCGCUUUGUAGGAUUCG-3'. All siRNA duplexes (Thermo Fisher Scientific) were transfected at a final concentration of 100 nM using Lipofectamine RNAiMAX (Invitrogen) according to the manufacturer's instructions for U2OS and BJ cells.

Cell culture

Human U2OS osteosarcoma cells and primary BJ fibroblasts were cultured in DME containing 10% fetal bovine serum. U2OS derivative cell lines expressing NLS-GFP-tagged hFbh1 constructs in a DOX-inducible fashion from pcDNA4/TO-NLS-GFP-hFbh1 vectors were generated and

maintained as described previously (Mailand et al., 2007). IR (6 Gy) was delivered using an x-ray generator (150 kV; 15 mA; dose rate, 2.18 Gy/min; HF160; Pantak). To induce local UV damage, cells grown on coverslips were irradiated with 100 J/m² UV-C light in a Stratalinker (Agilent Technologies) through a polycarbonate filter with 5- μ m pores (Millipore). Drugs used in this study included 1 μ g/ml DOX (EMD), 1 mM HU (Sigma-Aldrich), and 10 μ M BrdU (Sigma-Aldrich).

Immunochemical methods

Immunoblotting, immunoprecipitation, and immunofluorescence were performed as described previously (Mailand et al., 2006). To visualize generation of ssDNA upon HU treatment, cells were preincubated with BrdU for 24 h and subjected to BrdU immunofluorescence under nondenaturing conditions. To remove soluble proteins before immunofluorescence, cells grown on coverslips were preextracted for 5 min with ice-cold CSK buffer (10 mM Pipes, pH 6.8, 300 mM sucrose, 100 mM NaCl, and 1.5 mM MgCl₂) supplemented with 0.5% Triton X-100 before fixation with 4% paraformaldehyde. To obtain chromatin-enriched cellular fractions, cells were lysed in CSK buffer supplemented with 0.5% Triton X-100. Cell pellets were washed once with CSK buffer, resuspended in 0.2 M HCl, and incubated at 4°C for 2 h. The supernatant represented the chromatin-enriched fraction. A rabbit polyclonal antibody to hFbh1 was raised against a peptide spanning amino acids 168–182 of hFbh1 (Eurogentec). Rabbit polyclonal Rad51C antibody was provided by R. Kanaar (Erasmus Medical Center, Rotterdam, Netherlands). Other antibodies used in this study included mouse monoclonals to RPA (clone 9H8; NeoMarkers), BrdU (GE Healthcare), and Skp1 (Transduction Laboratories), rabbit polyclonals to Rad51 (H-92; Santa Cruz Biotechnology, Inc.), γ -H2AX (Millipore), cyclin A (H-432; Santa Cruz Biotechnology, Inc.), full-length GFP (Santa Cruz Biotechnology, Inc.), and human autoantibody to proliferating cell nuclear antigen (Immuno Concepts). EdU (5-ethynyl-2'-deoxyuridine) labeling was performed by incubating cells with 10 μ M EdU (Invitrogen) for 30 min followed by fluorescent staining according to the manufacturer's instructions.

Microscopy

Acquisition of confocal images was done essentially as described previously (Bekker-Jensen et al., 2006) using a confocal microscope (LSM 510; Carl Zeiss, Inc.) fitted with a PPlan Neofluar 40 \times NA 1.3 oil immersion objective (Carl Zeiss, Inc.). Laser microirradiation to generate DSBs in defined nuclear volumes was performed as described previously (Bekker-Jensen et al., 2006). For three-color imaging, GFP signals were combined with secondary antibodies coupled to AlexaFluor dyes with excitation wavelengths of 568 and 647 nm. Image acquisition and processing were performed with LSM 510 software (Carl Zeiss, Inc.). Quantification of Rad51 foci and BrdU was performed using custom-made macro routines. In brief, images were acquired using a fluorescence microscope (Axio-plan II; Carl Zeiss, Inc.) equipped with a Plan Neofluar 40 \times 1.3 oil immersion objective. Exposure time, binning, and settings of the microscope and light source were kept constant for all the samples. Photoshop (Adobe) was used to select single cells based on either EdU (for Rad51 foci) or DAPI (for BrdU staining). Each selected cell was subsequently analyzed using ImageJ software (National Institutes of Health) to measure the signal-integrated density of either Rad51 or BrdU staining. The numerical data were further processed in Excel (Microsoft) by mathematical operations, and statistical analysis of paired datasets was performed using *t* test (Prism; GraphPad Software, Inc.). The entire procedure was described previously in Mistrik et al. (2009).

EMSA

EMSA was performed essentially as described previously (Modesti et al., 2007). In brief, bacterially purified GST-hFbh1 constructs were incubated with ³²P-labeled ssDNA or dsDNA probes (2 nM) produced by standard methods in binding buffer (20 mM Tris-HCl, pH 7.4, 50 mM KCl, 0.1 mg/ml BSA, and 2 mM DTT) at 30°C for 15 min. Samples were resolved on native TBE polyacrylamide gels, dried, and visualized by autoradiography. DNA probes used in EMSA were X0-1, 5'-GACGCTGCCGAATTCTACCACTGCCCTGCTAGGACATCTTTGCCACCTGCAGGTTACCC-3'; and X0-1c, 5'-GGGTGAACCTGCAGGTGGGCAAGATGTCCTAGCAAGGCACTGTAGAATTCGGCAGCGTC-3'.

HR assay

HR rates were measured essentially as described previously (Sartori et al., 2007). In brief, a U2OS derivative cell line harboring an integrated HR reporter construct (DR-GFP) was cotransfected with plasmids expressing RFP, I-SceI, and, where indicated, hFbh1 for 48 h. Transfection of RFP

alone served as a reference for the absence of HR. Cells were collected by trypsinization and subjected to flow cytometric analysis of GFP and RFP. The extent of I-SceI-induced HR was measured as the ratio between the GFP and RFP signal.

SCC assay

Cells were incubated in the presence of 10 μ M BrdU for 46 h, after which 1 μ g/ml colcemide (Invitrogen) was added to the medium for an additional 2 h. Cells were harvested by trypsinization, resuspended in 75 mM KCl hypotonic buffer, and incubated at 37°C for 25 min. After centrifugation, cell pellets were incubated with fixative (75% methanol and 25% acetic acid) for 10 min, washed twice, and mitotic spreads were prepared by dropping the cell suspension in fixative on microscopy glass slides covered with water and allowed to air dry for at least 48 h in the dark. For chromatin staining, slides were immersed in Acridine orange (0.1 mg/ml in water; Invitrogen) for 3 min, washed thoroughly in water, and incubated in Sorenson buffer, pH 6.8 (0.1 M Na_2HPO_4 and 0.1 M NaH_2PO_4), for 3 min. Finally, slides were dried and analyzed by confocal microscopy.

Online supplemental material

Fig. S1 shows characterization of GFP-hFbh1-expressing cell lines, Fig. S2 shows characterization of hFbh1 mutants, and Fig. S3 shows efficiency of RNAi-mediated knockdown of hFbh1 in BJ fibroblasts. Online supplemental material is available at <http://www.jcb.org/cgi/content/full/jcb.200812138/DC1>.

We thank Dr. Yeon-So Seo for providing reagents.

This work was supported by grants from the Danish Cancer Society, the Danish National Research Foundation, the Danish Research Council, the Czech Ministry of Education (MSMT6198959216), the Grant Agency of the Czech Academy of Sciences (IAA501370902), the Lundbeck Foundation (R13-A1287), the European Commission (integrated projects "DNA Repair" and "GENICA"), and the John and Birthe Meyer Foundation.

Submitted: 22 December 2008

Accepted: 7 August 2009

References

- Barber, L.J., J.L. Youds, J.D. Ward, M.J. McIlwraith, N.J. O'Neil, M.I. Petalcorin, J.S. Martin, S.J. Collis, S.B. Cantor, M. Auclair, et al. 2008. RTEL1 maintains genomic stability by suppressing homologous recombination. *Cell*. 135:261–271.
- Bekker-Jensen, S., C. Lukas, R. Kitagawa, F. Melander, M.B. Kastan, J. Bartek, and J. Lukas. 2006. Spatial organization of the mammalian genome surveillance machinery in response to DNA strand breaks. *J. Cell Biol.* 173:195–206.
- Branzei, D., and M. Foiani. 2007. RecQ helicases queuing with Srs2 to disrupt Rad51 filaments and suppress recombination. *Genes Dev.* 21:3019–3026.
- Bugreev, D.V., X. Yu, E.H. Egelman, and A.V. Mazin. 2007. Novel pro- and anti-recombination activities of the Bloom's syndrome helicase. *Genes Dev.* 21:3085–3094.
- Chiolo, I., M. Saponaro, A. Baryshnikova, J.H. Kim, Y.S. Seo, and G. Liberati. 2007. The human F-Box DNA helicase FBH1 faces *Saccharomyces cerevisiae* Srs2 and postreplication repair pathway roles. *Mol. Cell. Biol.* 27:7439–7450.
- Gravel, S., J.R. Chapman, C. Magill, and S.P. Jackson. 2008. DNA helicases Sgs1 and BLM promote DNA double-strand break resection. *Genes Dev.* 22:2767–2772.
- Groth, A., A. Corpet, A.J. Cook, D. Roche, J. Bartek, J. Lukas, and G. Almouzni. 2007. Regulation of replication fork progression through histone supply and demand. *Science*. 318:1928–1931.
- Hu, Y., S. Raynard, M.G. Sehorn, X. Lu, W. Bussen, L. Zheng, J.M. Stark, E.L. Barnes, P. Chi, P. Janscak, et al. 2007. RECQL5/Recql5 helicase regulates homologous recombination and suppresses tumor formation via disruption of Rad51 presynaptic filaments. *Genes Dev.* 21:3073–3084.
- Kim, J.H., J. Kim, D.H. Kim, G.H. Ryu, S.H. Bae, and Y.S. Seo. 2004. SCFhFBH1 can act as helicase and E3 ubiquitin ligase. *Nucleic Acids Res.* 32:2287–2297.
- Kohzaki, M., A. Hatanaka, E. Sonoda, M. Yamazoe, K. Kikuchi, N. Vu Trung, D. Szüts, J.E. Sale, H. Shinagawa, M. Watanabe, and S. Takeda. 2007. Cooperative roles of vertebrate Fbh1 and Blm DNA helicases in avoidance of crossovers during recombination initiated by replication fork collapse. *Mol. Cell. Biol.* 27:2812–2820.
- Krejci, L., S. Van Komen, Y. Li, J. Villemain, M.S. Reddy, H. Klein, T. Ellenberger, and P. Sung. 2003. DNA helicase Srs2 disrupts the Rad51 presynaptic filament. *Nature*. 423:305–309.
- Mailand, N., S. Bekker-Jensen, J. Bartek, and J. Lukas. 2006. Destruction of Claspin by SCFbetaTrCP restrains Chk1 activation and facilitates recovery from genotoxic stress. *Mol. Cell*. 23:307–318.
- Mailand, N., S. Bekker-Jensen, H. Fastrup, F. Melander, J. Bartek, C. Lukas, and J. Lukas. 2007. RNF8 ubiquitylates histones at DNA double-strand breaks and promotes assembly of repair proteins. *Cell*. 131:887–900.
- Maluf, N.K., C.J. Fischer, and T.M. Lohman. 2003. A dimer of *Escherichia coli* UvrD is the active form of the helicase in vitro. *J. Mol. Biol.* 325:913–935.
- Mistrik, M., L. Oplustilova, J. Lukas, and J. Bartek. 2009. Low-dose DNA damage and replication stress responses quantified by optimized automated single-cell image analysis. *Cell Cycle*. 8:2592–2599.
- Modesti, M., M. Budzowska, C. Baldeyron, J.A. Demmers, R. Ghirlando, and R. Kanaar. 2007. RAD51AP1 is a structure-specific DNA binding protein that stimulates joint molecule formation during RAD51-mediated homologous recombination. *Mol. Cell*. 28:468–481.
- Morishita, T., F. Furukawa, C. Sakaguchi, T. Toda, A.M. Carr, H. Iwasaki, and H. Shinagawa. 2005. Role of the *Schizosaccharomyces pombe* F-Box DNA helicase in processing recombination intermediates. *Mol. Cell. Biol.* 25:8074–8083.
- Osman, F., J. Dixon, A.R. Barr, and M.C. Whitby. 2005. The F-box DNA helicase Fbh1 prevents Rhp51-dependent recombination without mediator proteins. *Mol. Cell. Biol.* 25:8084–8096.
- Rodrigue, A., M. Lafrance, M.C. Gauthier, D. McDonald, M. Hendzel, S.C. West, M. Jasin, and J.Y. Masson. 2006. Interplay between human DNA repair proteins at a unique double-strand break in vivo. *EMBO J.* 25:222–231.
- Sakaguchi, C., T. Morishita, H. Shinagawa, and T. Hishida. 2008. Essential and distinct roles of the F-box and helicase domains of Fbh1 in DNA damage repair. *BMC Mol. Biol.* 9:27.
- San Filippo, J., P. Sung, and H. Klein. 2008. Mechanism of eukaryotic homologous recombination. *Annu. Rev. Biochem.* 77:229–257.
- Sartori, A.A., C. Lukas, J. Coates, M. Mistrik, S. Fu, J. Bartek, R. Baer, J. Lukas, and S.P. Jackson. 2007. Human CtIP promotes DNA end resection. *Nature*. 450:509–514.
- Sung, P., and H. Klein. 2006. Mechanism of homologous recombination: mediators and helicases take on regulatory functions. *Nat. Rev. Mol. Cell Biol.* 7:739–750.
- Veaute, X., J. Jeusset, C. Soustelle, S.C. Kowalczykowski, E. Le Cam, and F. Fabre. 2003. The Srs2 helicase prevents recombination by disrupting Rad51 nucleoprotein filaments. *Nature*. 423:309–312.
- Wu, L., and I.D. Hickson. 2006. DNA helicases required for homologous recombination and repair of damaged replication forks. *Annu. Rev. Genet.* 40:279–306.
- Zhu, Z., W.H. Chung, E.Y. Shim, S.E. Lee, and G. Ira. 2008. Sgs1 helicase and two nucleases Dna2 and Exo1 resect DNA double-strand break ends. *Cell*. 134:981–994.